

## Spectrally coded multiplexing in a strain sensor system based on carrier-modulated fibre Bragg gratings

**Author/Contributor:**

Childs, Paul; Whitbread, Trevor; Peng, Gang-Ding

**Publication details:**

Proceedings of SPIE Vol 5634  
pp. 204-210

**Event details:**

Photonic Asia Conference on Information Optics and Photonics Technology  
Beijing, China

**Publication Date:**

2004

**Publisher DOI:**

<http://dx.doi.org/10.1117/12.580641>

**License:**

<https://creativecommons.org/licenses/by-nc-nd/3.0/au/>

Link to license to see what you are allowed to do with this resource.

Downloaded from <http://hdl.handle.net/1959.4/43061> in <https://unsworks.unsw.edu.au> on 2022-06-28

# Spectrally coded multiplexing in a strain sensor system based on carrier-modulated fibre Bragg gratings

Paul Childs, Trevor Whitbread and Gang-Ding Peng\*  
Photonics & Optical Communications Group  
School of Electrical Engineering & Telecommunications,  
University of New South Wales  
Sydney 2052, Australia  
\*Email: G.Peng@unsw.edu.au

## Abstract

In order to increase the number of channels available to a grating based strain sensor system specialised gratings were designed that would allow the sensor system to be able to distinguish between a number of gratings located in the one WDM channel independently of the amount by which they overlap each other in the wavelength domain. Distinguishing between gratings is achieved by inscribing a carrier frequency in the grating spectrum, so that each grating can be addressed in the Fourier domain via the spectral information centred around the inscribed carrier frequency. Tests performed on the gratings successfully show the ability to distinguish between three spectrally overlapping gratings. The calculated value for Young's modulus,  $72\pm 3\text{GPa}$ , was found to be in keeping with the standard value of  $70.3\text{GPa}$  for fused silica.

Keywords: Key words: Optical fibre sensors, Fibre Bragg Gratings, harmonic analysis, multiplexing.

## 1. Introduction

Fibre optic sensing technology has received an increasing amount of attention in the past decade. Fibre optic sensors offer the advantage over conventional electrical sensors largely due to their non-invasiveness as well as their virtual immunity from electro-magnetic interference. Of fibre optic sensors, Fibre Bragg Gating (FBG) sensors have shown the most potential in a wide range of applications due to their passive nature, as well as the ability to fabricate them with almost arbitrary spectral shapes. The key issues for designing a Fibre Bragg Grating based strain sensor system are strain resolution, system update rate and the channel count. Traditionally the most important of these issues is that of having a very fine strain resolution; i.e. to make a very accurate sensor. However, for sensors which are intended for use in the monitoring of large scale structures, of which the greatest amount of interest in optical strain sensors has been shown, then the most crucial of these issues will be the channel count. In order to reduce the cost of having a sensor system for each channel (or a few of the channels) required it will be important to multiplex the sensors together, thus sharing out the cost of the more expensive components.

The conventional techniques for multiplexing FBG's are Wavelength Division and Time Domain Multiplexing, i.e. WDM & TDM respectively. There are limitations to the use of TDM and WDM however. TDM may require the use of long delay lines which, if embedded, would reduce the structural integrity of the host material. Hence the use of a TDM architecture would be undesirable for use in many civil engineering applications. WDM, although useful, has its limitations. Typically about 50 nm (corresponding to 1520-1570 nm) of spectrum is available for use by most optical equipment. If a system is required to be able to measure from 0 to 5000  $\mu\text{e}$  on each sensor, this would give an upper limit of 8 WDM channels. This is clearly insufficient for use in monitoring a large scale structure.

The method we demonstrate is to make use of an excess sampling (which would otherwise lead to having a finer strain resolution) in order to distinguish between a number of gratings that are partially or completely overlapped. This is achieved by writing the gratings such that they have an inscribed carrier signal. The system used to interrogate the gratings uses either a swept laser source or a tuneable filter (as in [1]) so as to represent the reflected wavelength spectrum as a time series signal. In taking the Fourier transform of this data series, each sensor of the one WDM channel

will have a frequency band assigned to it. This is known as compact support. In this way, it is possible to further demultiplex gratings in the Fourier domain just as the initial demultiplexing was done in the wavelength domain.

## 2. Theoretical Considerations

A complete theoretical description has already been given in [2] so we will only present the key results here. The requirement that a grating have a reflection spectrum that is positive real valued and that its Fourier transform has compact support (of which there exists a subset that is non-overlapping w.r.t. the support of the other gratings) leads to the natural choice for its Fourier transform as:

$$M_{\kappa c}(s) \propto \left[ 2\delta(s) + \delta\left(s - \frac{j+\eta}{2n+1}\right) + \delta\left(s + \frac{j+\eta}{2n+1}\right) \right] * \wedge\left(\frac{4n+2}{1-\zeta}s\right),$$

where  $n$  represents the maximum number of gratings per wavelength channel,  $\zeta$  is a parameter giving the spacing between channels,  $\eta$  gives the additional spacing around the zeroth order peak,  $\delta(s)$  is the dirac delta function,

$\wedge(s) = \chi(|s|)(1-|s|)$  is the triangular hat function and the characteristic function  $\chi(s) = 1$  if  $0 \leq s \leq 1$ , otherwise it is equal to zero. A graph of  $M_2(s)$  is given in figure 1.

Taking the inverse Fourier transform and compensating for spectral shadowing gives the required grating reflection spectrum:

$$R_{k,j}(\lambda) = 1 - 10^{-\frac{L_{k,j}}{10} \cos^2\left(\frac{(j+\eta)\pi(\rho(\lambda-\lambda_{0,k}))}{2n+1}\right) \text{sinc}^2\left(\frac{(1-\zeta)\rho(\lambda-\lambda_{0,k})}{4n+2}\right)}$$

where  $\rho$  is the sampling density and  $L_{k,j}$  is the peak loss of grating  $(k,j)$ . In order to process the signal from an array of such gratings so as to find the response of grating  $(k,j)$ , firstly the spectrum is divided up into segments in the wavelength domain and the segment with index  $\kappa=k$  selected. Then the reverse procedure of the above analysis is applied and a segment of the resultant spectrum  $M(s)$  with index  $\kappa=j$  is selected. The strain can thus be found from the weighted

averaged differential phase spectrum  $\overline{\Delta d\Phi}_{\kappa,\kappa c}^+$  as:

$$\mathcal{E}_{\kappa,\kappa c}^+ = \frac{1}{\rho\Gamma\lambda_0} \left( \frac{\overline{\Delta d\Phi}_{\kappa,\kappa c}^+}{2\pi} - \xi - o \right)$$

where  $\lambda_0$  is the operating wavelength,  $\xi$  and  $o$  are parameters defining the amount of channel isolation in the wavelength domain and  $\Gamma$  is the strain-wavelength conversion coefficient given as 0.78 by Meltz et al [3].

## 3. Results

The required gratings were fabricated by Redfern Optical Components. However, due to a numerical error on the part of the primary author, the specifications given for the grating envelopes were half as wide as what was required by the theory above. As a result the corresponding indices,  $\{j\}$ , of the gratings were  $\{1, 2, 2.5\}$  instead of  $\{2, 4, 5\}$ . All measurements of the sensors were carried out using a swept wavelength source operating at a power of 0.5 mW. Figure 2 shows the measured reflection spectrum of the grating with the modulation index  $j=2$ .

The three gratings were spliced together in series with the  $j=2$  grating being the closest to the source, then the  $j=1$  grating and then the  $j=2.5$  grating. The  $j=2$  and  $j=1$  gratings were kept strain free and various loads were applied to the  $j=2.5$  sensor. The measured reflection spectra for the cases of zero load and a small load of 7.7 MPa are shown in figures 3 and 4 respectively.

The spectrum of the combined grating array was processed according to that given in [2], but with two exceptions. Firstly, as only three weak gratings were used, the corrections for spectral shadowing were not applied and secondly, in order to provide greater flexibility, the weight used for averaging the differential phase spectrum corresponded to the magnitude spectrum rather than being a fixed Gaussian. The magnitude of the Fourier spectrum for the case of zero

strain is shown in figure 5. It can be seen that the three peaks corresponding to each of the gratings match well to what is theoretically expected.

The sample bounds for demultiplexing in the Fourier domain were taken to be the intervals [80,130], [175,225] and [250,275] out of a total data range of 15942 samples. As the peaks seen in figure 5 lie at the positions 102, 204 and 254, the latter two intervals thus contain part of the power spectrum of the grating associated with the other.

The strain vs. applied stress obtained from taking the weighted average of the differential phase spectrum over these intervals is shown in figure 6. The theoretical response has also been included for comparison. In calculating the applied stress it was assumed that the stress was taken up entirely by the glass fibre and that the plastic coating over the region of the fibre where the sensors were located was essentially stress free. The amount measurement error, obtained from the variation in strain of the gratings that were kept strain free, was found to be  $\pm 8\mu\epsilon$ . A linear regression was applied to the data and is plotted in figure 7. From the gradient of the fit, Young's modulus of the fibre was determined to be  $72\pm 3\text{GPa}$ .

#### 4. Analysis

From a cursory overview of the theory, it would be expected that gratings 2 and 2.5 would exhibit a large amount of crosstalk due to the overlapping of the spectra in the Fourier domain. That this is not the case suggests that we need to examine what is going on further.

The behaviour of the resultant Fourier signal that occurs when two channels are overlapping in the Fourier domain can be visualised by adding together two vectors of different lengths rotating at different angular velocities. The length of the vectors represents the magnitude of the Fourier signal and the direction of the vector is due to the phase component of the Fourier signal. Due to the Fourier shift relation, the angular velocity of the vector will be a linear function of the applied strain. Averaged over a large number of cycles, the angular velocity of the pair will be predominantly due to the angular velocity of the longer of the two.

This is shown in figure 8 where a spirograph has been used to trace out the position of the sum of the two vectors when the ratio of the length and angular velocities of the vectors are arbitrarily chosen to be 89:23 and 9:89 respectively. In this case the true angular position will deviate from the angular position obtained by considering the behaviour of the larger of the vectors alone by  $\pm 0.25$  radians. It can be seen that by taking the average over a large number of revolutions the contribution of the effect of the precession of the second vector to the relative error, and thus to the amount of crosstalk inherent in the system, will become insignificant. In this simplified model we have ignored the fact that the magnitude of the two lengths will change over the region of interest. Nonetheless, the qualitative behaviour would be unchanged in making a more thorough treatment.

#### 5. Conclusion

Three gratings were successfully demultiplexed, even when partially or completely overlapped. The resultant stress-strain response of the sensors of  $72\pm 3\text{GPa}$  was in good agreement with the given value of  $70.3\text{GPa}$ . Despite the relaxing of the condition of compact support it was found that the crosstalk was nonetheless sufficiently suppressed anyway.

#### 6. Acknowledgement

The authors would like to thank Antonio Brotons and Jesús Ammar for their collaboration in the tests.

#### Reference

1. A.D. Kersey, T.A. Berkoff, & W.W. Morey "Multiplexed fiber Bragg grating strain-sensor system with a fiber Fabry-Perot wavelength filter," *Optics Lett.* **18**, 1370-1372 (1993).
2. P. Childs, "A FBG Sensing System utilising both WDM and a novel Harmonic Division Scheme," accepted to *J. of Lightwave Tech.*
3. G. Meltz, W.W. Morey, W.H. Glenn and J.D. Farina, 163 *Proc. OFS 88*.

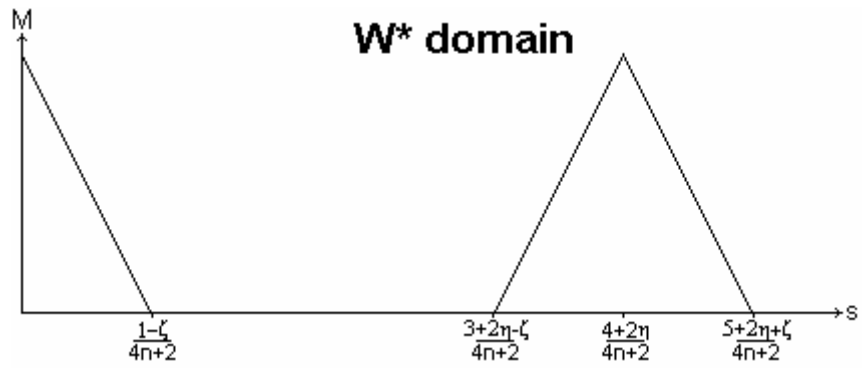


Fig.1. graph of  $M_2(s)$

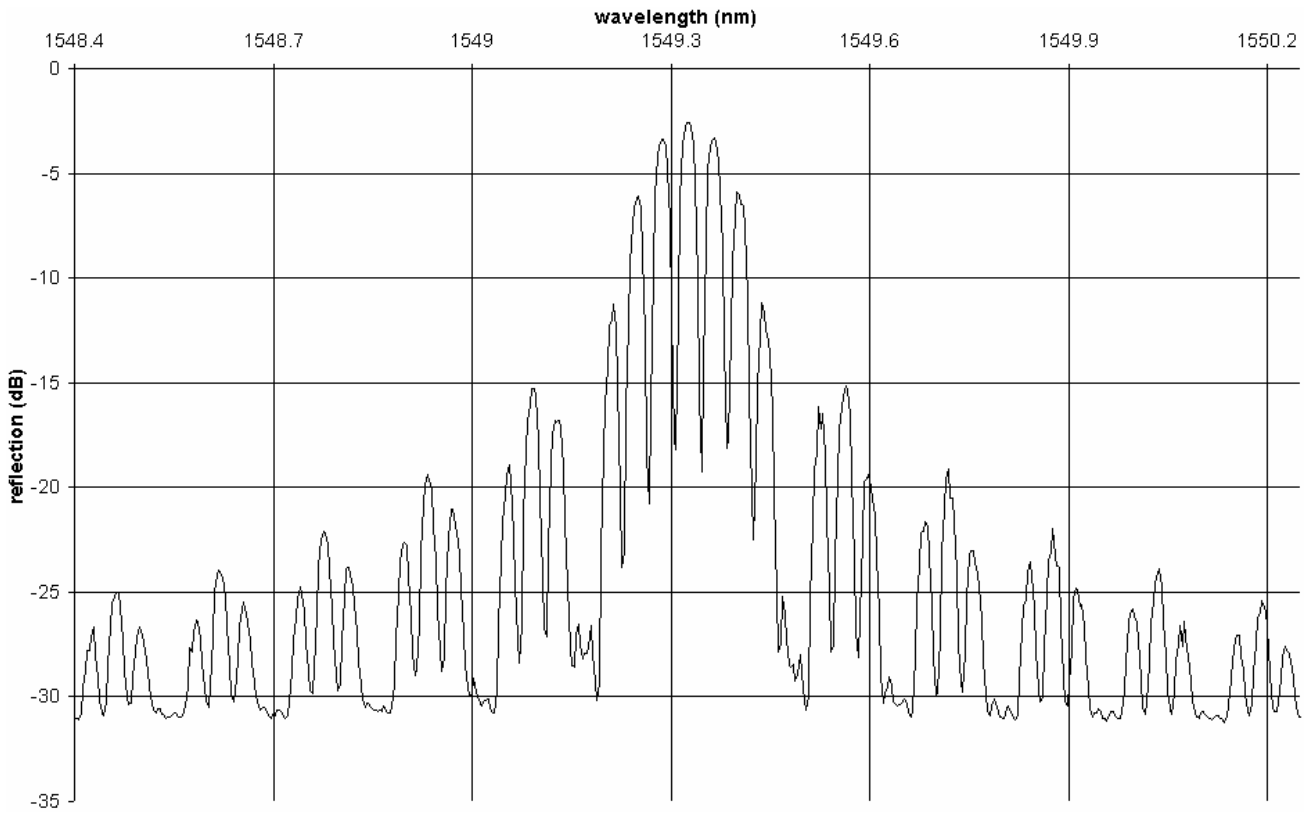


Fig.2. Measured reflectivity spectrum of the grating corresponding to  $j=2$ .

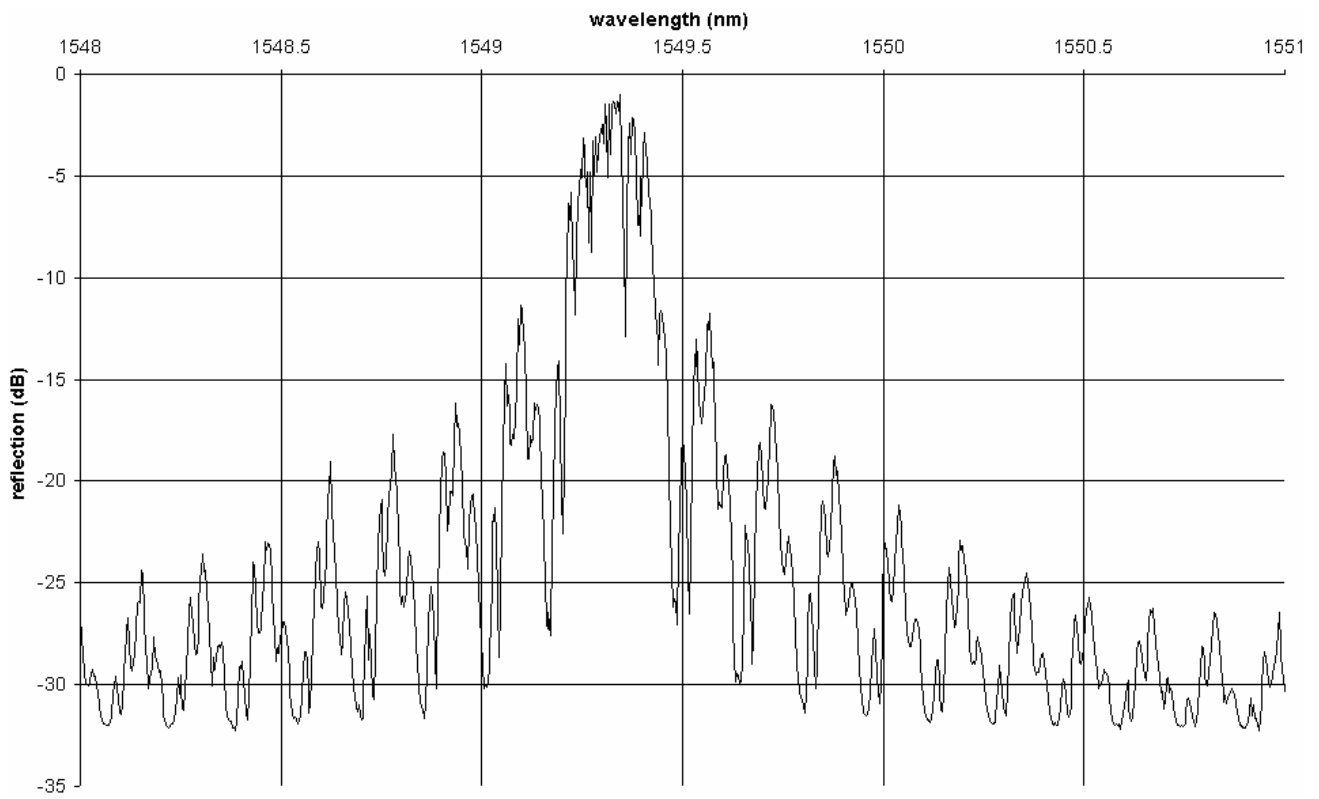


Fig.3. Spectrum of the combined grating array with no stress applied to the sensors.

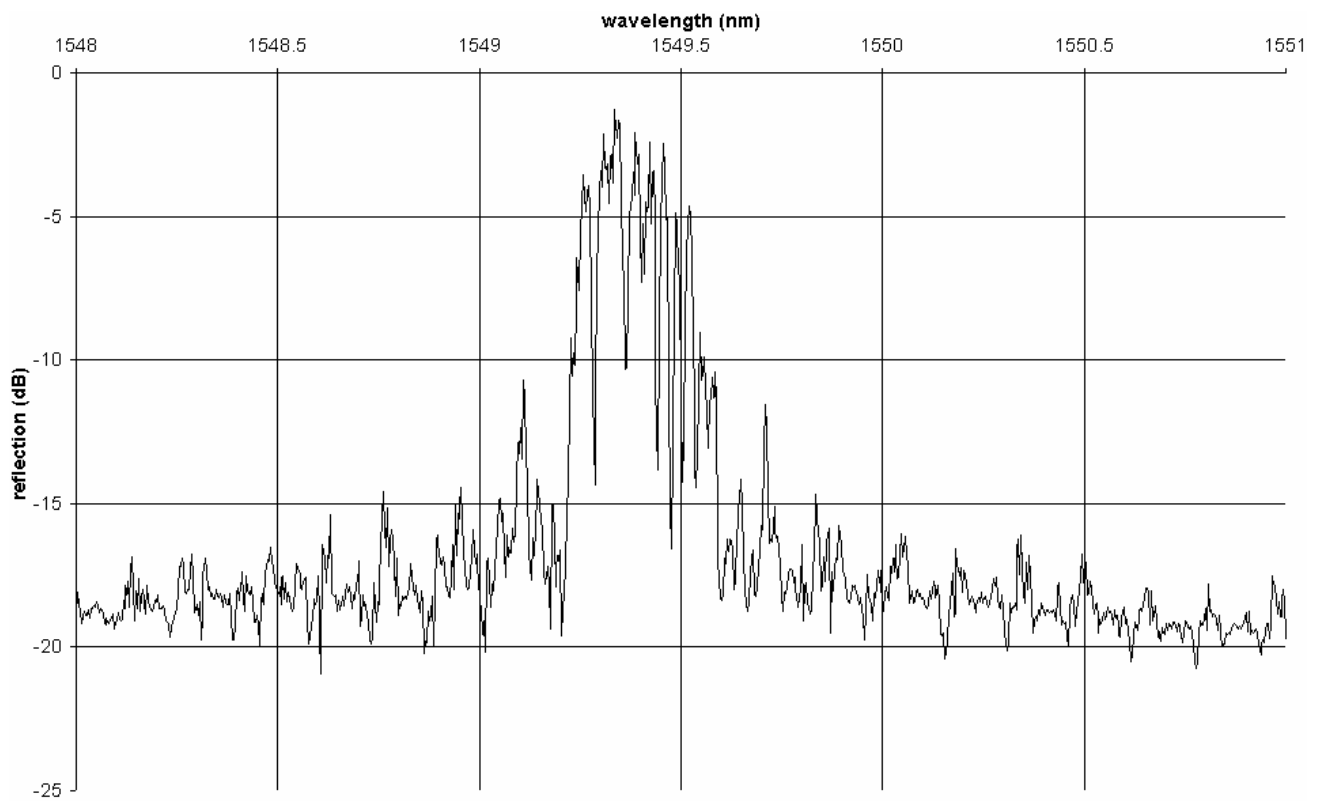


Fig.4. Spectrum of the combined grating array with 7.7 MPa of stress applied to the  $j=2.5$  sensor.

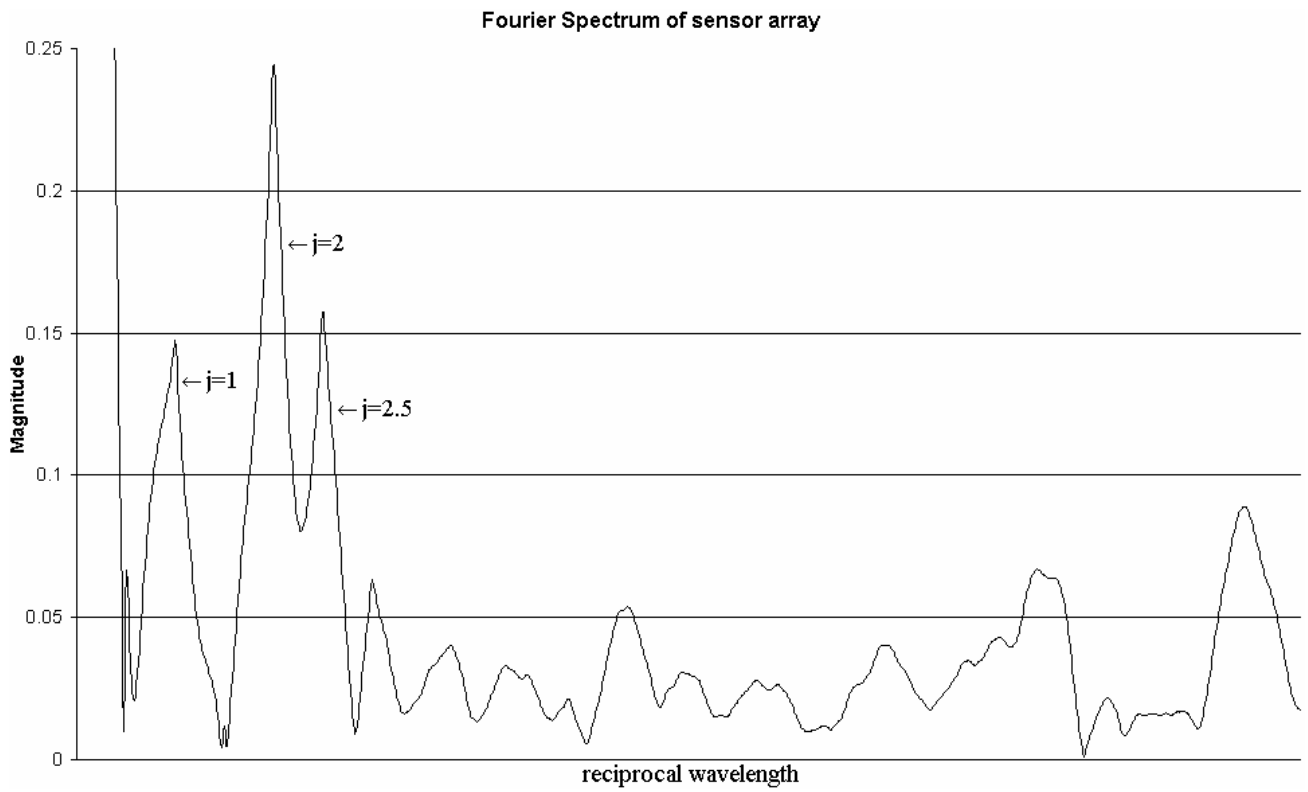


Fig.5. Fourier Domain spectrum of the grating array.

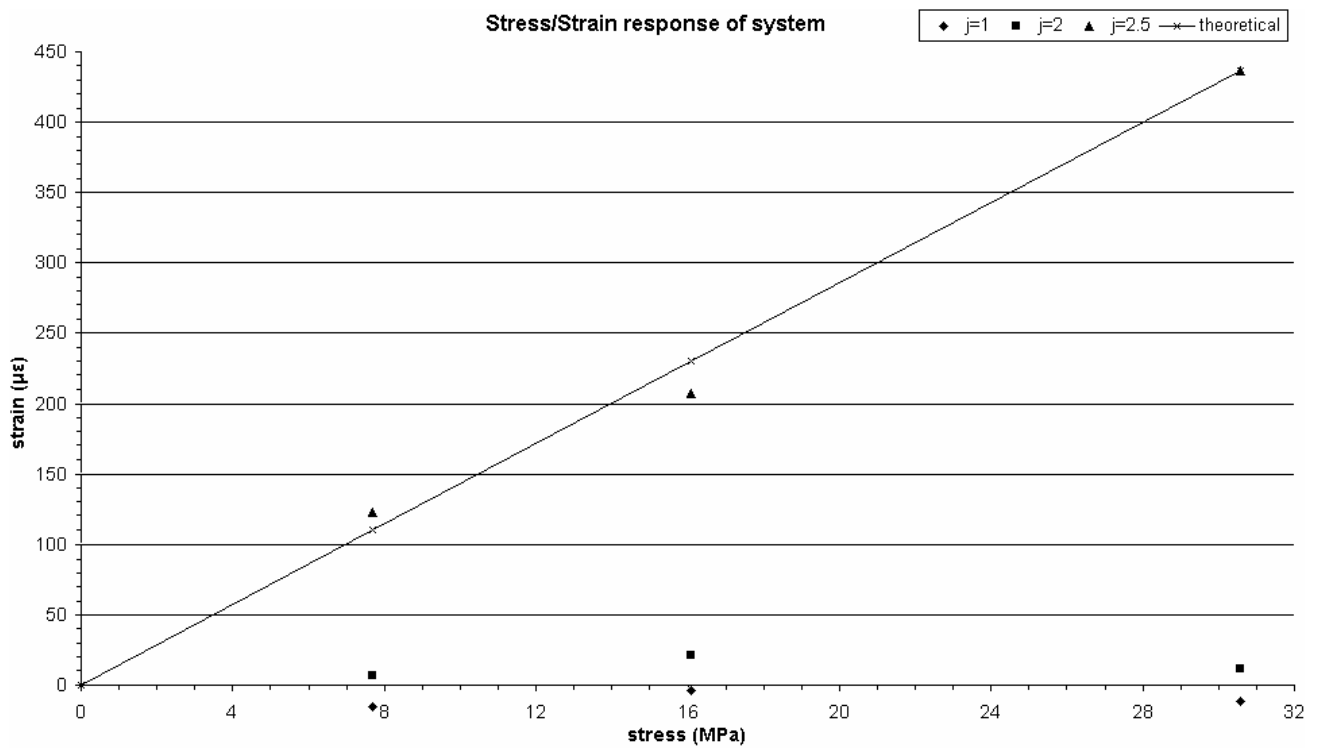
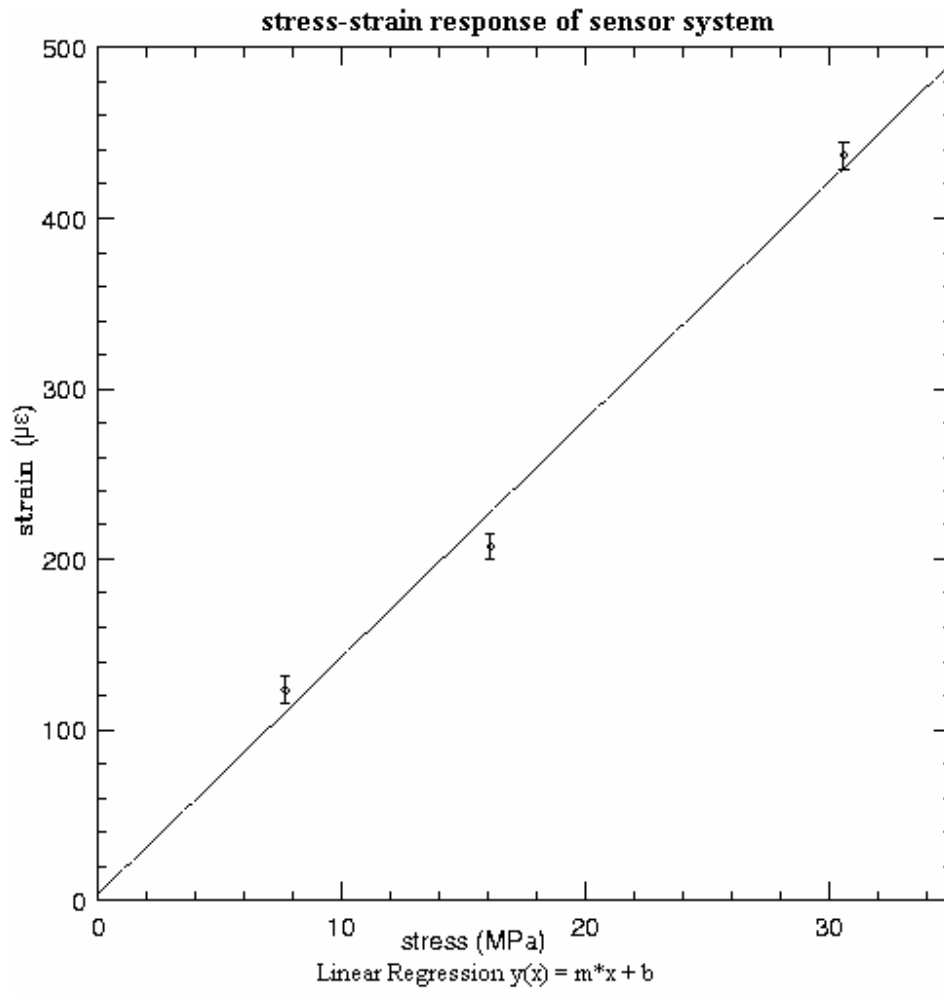


Fig.6. Measured strain vs. stress applied to the  $j=2.5$  grating.



<b>m</b>	<b>b</b>	<b>dm</b>	<b>db</b>	<b>chi<sup>2</sup></b>	<b>q</b>
13.9364	3.1861	0.488307	9.98689	9.65691	0.00188641

Fig.7. Linear fit for the data obtained in figure 6.

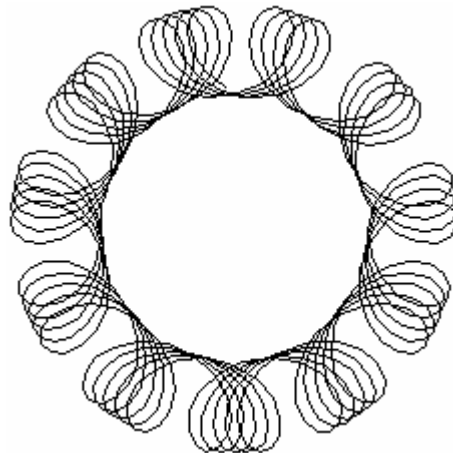


Fig.8. Locus of the sum of two rotating vectors with  $|x_1| = \frac{89}{23}|x_2|$  and  $\omega_1 = \frac{9}{89}\omega_2$ .